

EPJ manuscript No.
(will be inserted by the editor)

Scattering of a sound wave by a vibrating surface

Nicolás Mujica, Régis Wunenburger, Stéphan Fauve

Laboratoire de Physique Statistique, Ecole Normale Supérieure, UMR 8550, 24, rue Lhomond, 75005 Paris, France

March 16, 2003

Abstract. We report an experimental study of the scattering of a sound wave of frequency f by a surface vibrating at frequency F . Both the Doppler shift at the vibrating surface and acoustic nonlinearities in the bulk of the fluid, generate the frequencies $f \pm nF$ (n integer) in the spectrum of the scattered wave. We show that these two contributions can be separated because they scale differently with respect to the vibration frequency and to the distance between the vibrating scatterer and the detector. We determine the parameter ranges in which one or the other mechanism dominates and present quantitative studies of these two regimes.

PACS. 43.25.+y Nonlinear acoustics – 43.20.Fn Scattering of acoustic waves – 43.58.+z Acoustical measurements and instrumentation

1 Introduction

A problem of interest in the discussion of nonlinear effects is how the boundary surfaces of the media affect the results. Generation of longitudinal waves from transverse ones in solids [1], first to second sound conversion in superfluid helium [2], second harmonic generation in optics [3], can result from both bulk nonlinearities and boundary conditions at interfaces. An essential question is thus, how can one distinguish between bulk and surface nonlinearities.

In particular, this problem arises when an acoustic wave of frequency f is reflected by a boundary vibrating at frequency F . The scattered signal being Doppler shifted, its spectrum involves peaks at frequencies $f \pm nF$ (n integer) [4]. The vibrating surface also emits an acoustic wave at frequency F that interacts with the high frequency one f through nonlinear terms in the conservation equations and in the equation of state. These also generate sum and difference frequencies [5,6]. Although Doppler shift and bulk nonlinearities lead to spectra with the same components of frequency, the amplitudes of the waves generated

through bulk nonlinearities increase with distance from the vibrating surface, thus it has been argued that they give the dominant contribution to the spectrum within a fraction of a wavelength of the scatterer's surface. It has been even claimed that the contribution of the Doppler effect might be undetectable [7]. This has been the subject of a strong theoretical controversy [4, 7]. In this letter, we present an experimental study of the spectral characteristics of an acoustic wave scattered by a vibrating piston. We show that there exists a wide parameter range in which the Doppler shift gives the dominant contribution to the spectrum of the scattered wave. We then study the cross-over to the bulk nonlinear regime.

2 Doppler shift versus bulk acoustic nonlinearities

The scattering of a wave by a vibrating surface, $\xi = A \sin \Omega t$ ($\Omega = 2\pi F$), has been widely studied theoretically, first in the case of electromagnetic waves [8] and then in acoustics [4]. A simple way to describe this process is to consider the Doppler shift of the high frequency wave scattered by the vibrating surface. We assume that this wave is emitted by a transducer located at a distance L from the plate, reflected normally and detected by the same transducer. Thus the scattered wave measured at time t , has been generated at time $t - \tau(t)$ and reflected at time $t - \tau(t)/2$. Writing that it propagated at velocity c gives

$$\tau(t) = \frac{2}{c} \left[L - \xi \left(t - \frac{\tau(t)}{2} \right) \right]. \quad (1)$$

The detected wave is thus of the form

$$p_s \propto \exp i\omega(t - \tau(t)). \quad (2)$$

If $A \ll L$, we have $\tau(t) \approx 2L/c$. In addition, if the velocity of the plate is small compared to the sound velocity c , $M \equiv A\Omega/c \ll 1$, we can substitute this value of τ in the vibration amplitude ξ in (2). We get the quasi-static approximation, which gives up to a constant phase factor

$$\begin{aligned} p_s &\propto \exp i\omega \left[t + \frac{2}{c} \xi \left(t - \frac{L}{c} \right) \right] \\ &\propto \exp i \left[\omega t + 2kA \sin \Omega \left(t - \frac{L}{c} \right) \right]. \end{aligned} \quad (3)$$

Consequently, we observe that the Doppler effect generates a phase modulation of scattered wave with a characteristic magnitude $\Delta\Phi_D = 2kA$ where A is the vibration amplitude and k the wave number of the high frequency wave. Using

$$\begin{aligned} &\exp i \left[\omega t + (2kA) \sin \Omega \left(t - \frac{L}{c} \right) \right] \\ &= \exp(i\omega t) \sum_{n=-\infty}^{+\infty} J_n(2kA) \exp \left[in\Omega \left(t - \frac{L}{c} \right) \right], \end{aligned} \quad (4)$$

we observe that the amplitude of the peak at pulsation $\omega \pm n\Omega$ is given by the modulus of the Bessel function of order n , $|J_n(2kA)|$ which scales like $(kA)^n$ for kA small.

Acoustic nonlinearities in the bulk of the fluid also generate a phase modulation of the high frequency wave [9]. There are two contributions, the nonlinear terms in the fluid equations and those in the equation of state. In the case of plane waves their effect can be understood as a modification of the high frequency wave propagation velocity c by an amount $\Delta c \propto V_\Omega \propto P_\Omega/\rho c$ where V_Ω (resp. P_Ω) is the typical amplitude of the velocity (resp. the pressure) modulation related to the low frequency wave,

and ρ is the fluid density. When the two waves are counterpropagating, the nonlinearly generated waves remain small because of the absence of phase matching. On the contrary, when the two waves propagate in the same direction, the phase of the nonlinearly generated waves can remain locked to the ones of the parent waves and the effect is cumulative. After propagation over a distance L , the characteristic magnitude $\Delta\Phi_{NL}$ of the phase modulation due to bulk nonlinearities is $\Delta\Phi_{NL} \propto L\Delta k = L\omega\Delta c/c^2 \propto L\omega P_\Omega/\rho c^3$. A detailed calculation in the case of a perfect gas of adiabatic index γ gives $\Delta\Phi_{NL} = (1+\gamma)L\omega P_\Omega/2\rho c^3$ [9]. For a liquid, one should replace $(1+\gamma)/2$ by the acoustic nonlinear parameter $\epsilon = 1 + \rho(\partial c/\partial \rho)_S/2c$ [10]. The first term on the right hand side is due to the nonlinearity of the conservation equations whereas the second traces back to the equation of state.

Thus, both the Doppler effect and bulk nonlinearities generate a phase modulation of the high frequency wave by the low frequency one. However, the shifted peak amplitudes scale differently with the vibration parameters: they depend on the vibration amplitude A when the Doppler effect is dominant and on the low frequency pressure P_Ω when bulk nonlinearities are dominant. We emphasize that despite these different scalings, the Doppler effect cannot be singled out just by decreasing the amplitude of the waves. It results from boundary conditions at the moving interface which are nonlinear as can be easily seen by taking the Taylor expansion of the fields at the interface in the vicinity of $\xi = 0$. The successive powers of the vibration amplitude are then involved in the boundary

conditions, thus generating the frequencies $f \pm nF$. Nonlinearities arising from boundary conditions at free interfaces are very common in capillary-gravity waves, crystal growth and flame fronts.

The importance of the Doppler shift related to the effect of bulk nonlinearities is thus measured by the parameter

$$Y = \frac{\Delta\Phi_D}{\Delta\Phi_{NL}} = \frac{2\rho c^2 A}{\epsilon L P_\Omega}. \quad (5)$$

In the case of plane propagating waves ($P_\Omega = \rho c V_\Omega \propto \Omega A$), we have $Y \propto A/L$ where A is the wavelength of the low frequency wave.

3 Experiments in water

Experiments have been performed both in air and in water, in different geometrical configurations. The set-up in air has been used to determine the dominant mechanism that generates sum and difference frequencies, the Doppler effect versus bulk acoustic nonlinearities, whereas the one in water allowed a quantitative study of the characteristics of the wave scattered from a vibrating piston when bulk nonlinearities are negligible compared to the Doppler effect.

Experiments in water have been performed in a tank of dimensions $72 \times 68 \times 55$ cm, thermally regulated at temperature $T = 15 \pm 0.2$ °C. Its lower boundary is covered with a layer of plastic foam (Plastiform's) in order to minimize the effect of multiple reflections. A square piston made of PMMA, of dimensions 15×15 cm and 10 mm thick, located beneath the upper surface of the water, is

driven sinusoidally by an electromagnetic vibration exciter (BK4808). Its motion is described by $\xi = A \sin \Omega t$ and is recorded using an accelerometer (BK 4393V) fixed on the piston. The range of vibration parameters is $3 \cdot 10^{-10} < A < 10^{-3}$ m, $30 < F < 6000$ Hz. A dual transducer (Panametrics D706), 13 mm in diameter, located at a distance $L = 18$ cm below the piston, generates an incident wave at frequency $f = 2.25$ MHz ($\omega = 2\pi f$) and records the wave scattered by the vibrating piston. Its power spectrum, computed by a spectrum analyzer (Agilent 3589A), is displayed in Fig. 1 for $F = 30$ Hz. We observe that the number and the amplitude of the peaks at frequencies $f \pm nF$ for $n \geq 1$ (n integer) first increases when the amplitude A is increased from zero (Fig. 1a, b). Fig. 2 shows that the normalized amplitudes $P_{\omega+\Omega}/P_{\omega}$ do not depend on the vibration frequency F in the range $30 < F < 3000$ Hz. A slight dependence on F begins to be observed only for $F = 6000$ Hz. Thus for $F < 3000$ Hz, the Doppler effect is dominant and bulk nonlinearities can be neglected. For kA small, the amplitude of the peak at frequency $f \pm nF$ ($n \geq 1$) increases like $(kA)^n$, as shown for $n = 1$ and $n = 2$. On the contrary, the amplitude of the component at frequency f of the scattered wave decreases and we observe that it almost vanishes for $2kA \approx 2.3$ (see Fig. 1c). It increases when A is increased further above $2kA \approx 2.3$, then decreases and vanishes again for $2kA \approx 5.4$. The same process occurs roughly periodically for the amplitude of each peak $f \pm nF$, as displayed in Fig. 3 for $n = 0, 1, 2, 3$. This behavior can be understood from Eq. (4). We observe in Fig. 3 that the agreement is rather good.

4 Experiments in air

Experiments in air are performed in a 1 m long tube made of PMMA, 56.5 mm in inner diameter. A cylindrical piston made of aluminium, 55.8 mm in diameter, is located at one end of the tube, $x = 0$ say, and is driven sinusoidally with amplitude A and frequency F as for the experiments in water. A transducer ITC 9072, 16 mm in diameter, located at position $x = L$, $0.3 < L < 1$ m, generates a wave at frequency $f = 150$ kHz, incident on the vibrating piston. The scattered wave is recorded by another ITC 9072 transducer, also located at $x = L$, 3 mm apart from the first one. We also measure at the same location $x = L$, the low frequency pressure P_{Ω} generated by the vibrating piston, using a PCB 103A pressure transducer with a flat response in the range 1 – 5000 Hz.

The power spectrum of the scattered wave is computed with a spectrum analyzer (Agilent 3589A). As for experiments in water, it displays peaks at frequencies $f \pm nF$ (n integer). The amplitude of the pressure at pulsation $\omega + \Omega$, $P_{\omega+\Omega}$, normalized by that of the wave scattered at pulsation ω , P_{ω} , is displayed in Fig. 4. Fig. 4a shows that at low enough frequency of the vibrating piston, $30 < F < 964$ Hz, $P_{\omega+\Omega}/P_{\omega}$ does not depend on Ω and increases linearly with the vibration amplitude A as for experiments in water. At higher vibration frequency, $1.2 < F < 4.5$ kHz, we observe a clear departure from the low frequency curve. On the contrary, when $P_{\omega+\Omega}/P_{\omega}$ is plotted as a function of the low frequency pressure P_{Ω} generated by the vibrating piston, we observe in Fig. 4b that the data collapse on a single curve at high F and depart from this curve at low

F . We thus observe that bulk nonlinearities become dominant at high frequency because the two waves interact on a larger number of low frequency wavelengths.

Another way to study the cross-over between the two regimes is to vary the distance L and frequency F for constant A ($A = 0.22 \mu\text{m}$), i.e. keeping the contribution of the Doppler effect constant. The measurements are displayed in Fig. 5 as a function of L/Λ . For L/Λ small enough, we observe that $P_{\omega+\Omega}/P_{\omega}$ is constant as it should be when the Doppler effect is dominant. When L/Λ is large, $P_{\omega+\Omega}/P_{\omega}$ increases with L/Λ on average, but also displays strong local maxima. We have checked that they correspond to acoustic resonances of the tube ($L/\Lambda \approx n/2$) for which P_{Ω} shows a maximum. According to Eq.(5) this strongly enhances the contribution of bulk nonlinearities. In order to take into account the contribution of P_{Ω} , we have plotted in the inset of Fig. 5 $P_{\omega+\Omega}/P_{\omega}$ as a function of the dimensionless parameter Y (see Eq. 5). For Y large, $P_{\omega+\Omega}/P_{\omega}$ does not depend on Y . When Λ is decreased for fixed L , such that Y becomes smaller than one, the cooperative effect of bulk nonlinearities becomes dominant and $P_{\omega+\Omega}/P_{\omega}$ increases like Y^{-1} . Note also that it is apparent in Fig. 5 that $P_{\omega+\Omega}/P_{\omega}$ first decreases when bulk nonlinearities become comparable to the contribution of the Doppler effect, i.e. when L/Λ is increased such that $Y \approx 1$. This clearly shows that these two contributions are not in phase as can be inferred from the fact that the amplitude of the Doppler shifted wave scales with the vibration amplitude whereas that of the nonlinearly shifted wave depends on the low frequency velocity field. The slight

decrease of the amplitude ratio thus results from interferences between the waves generated by Doppler shift and bulk nonlinearities. It may also involve a contribution of a cavity effect in our geometry.

Finally, it is interesting to compare the transition values of Y observed with air and water. In the water experiments, Y has been varied in the range $0.11 < Y < 22$ corresponding to $30 < F < 6000$ Hz. $Y \approx 1$ corresponds to $F \approx 700$ Hz whereas, as shown in section 3, the Doppler shift is still dominant at much higher frequencies. This shows that the criterion $Y \approx 1$ for the transition should be taken with care. It is roughly correct when the waves are one dimensional as for the experiments in air that have been performed in a tube. The experiments in water have been performed in non confined geometry and both the low and high frequency waves are slightly divergent. This decreases the strength of bulk nonlinearities and the Doppler shift thus remains dominant at higher Y i. e. higher frequencies.

5 Conclusion

We have thus clearly identified two scattering regimes: one for which the only contribution to the sum and difference frequencies comes from the Doppler shift by the vibrating piston, bulk nonlinearities being negligible, and another one for which the frequency shifted wave is dominantly generated by bulk acoustic nonlinearities. Both effects are intrinsically nonlinear and thus neither of them can be made dominant by varying only the vibration amplitude. However, they scale differently with vibration frequency

and with distance between the vibrating scatterer and the detector. It is thus possible to single out one of them but it is important to check carefully that the other one is negligible when one uses this scattering technique for nonintrusive measurements of vibration or for the determination of the nonlinear acoustic parameter of a fluid.

R. W. thanks the Centre National d'Etudes Spatiales for financial support. This work has been supported by contract No. 793/CNES/01/8601/00.

References

1. L. D. Landau and E. M. Lifshitz, *Theory of elasticity*, 3rd edition, Pergamon (Oxford, 1986); F. R. Rollins, L. H. Taylor and P. H. Todd, *Phys. Rev.* **136**, A 597 (1964).
2. S. Garrett, S. Adams, S. Putterman and I. Rudnick, *Phys. Rev. Lett.* **41**, 413 (1978); B. Castaing and P. Nozières, *J. Physique* **41**, 701 (1980).
3. Y. R. Shen, *The principles of nonlinear optics*, John Wiley and sons (New York, 1984); S. S. Jha, *Phys. Rev. Lett.* **15**, 412 (1965).
4. D. Censor, *J. Sound Vib.* **25**, 101 (1972), *J. Acoust. Soc. Am.* **76**, 1527 (1984), *J. Acoust. Soc. Am.* **79**, 181 (1986), *J. Acoust. Soc. Am.* **83**, 1223 (1988).
5. P. H. Rogers, *J. Sound Vib.* **28**, 764 (1973).
6. L. Naugolnykh and L. Ostrovsky, *Nonlinear wave processes in acoustics*, Cambridge University Press (Cambridge, 1998).
7. J. C. Piquette and A. L. van Buren, *J. Acoust. Soc. Am.* **76**, 880 (1984), *J. Acoust. Soc. Am.* **79**, 179 (1986), *J. Acoust. Soc. Am.* **80**, 1533 (1986), *J. Acoust. Soc. Am.* **83**, 1681 (1988).
8. A. M. Kovalev and V. N. Krasil'nikov, *Soviet Phys. Tech. Phys.* **7**, 19 (1962); D. Censor, *Phys. Rev. A* **35**, 2869 (1987).
9. V. A. Zverev and A. I. Kalachev, *Sov. Phys. Acoust.* **16**, 204 (1970).
10. R. T. Beyer, in *Nonlinear acoustics*, M. F. Hamilton and D. T. Blackstock eds., Academic Press (New York, 1998).

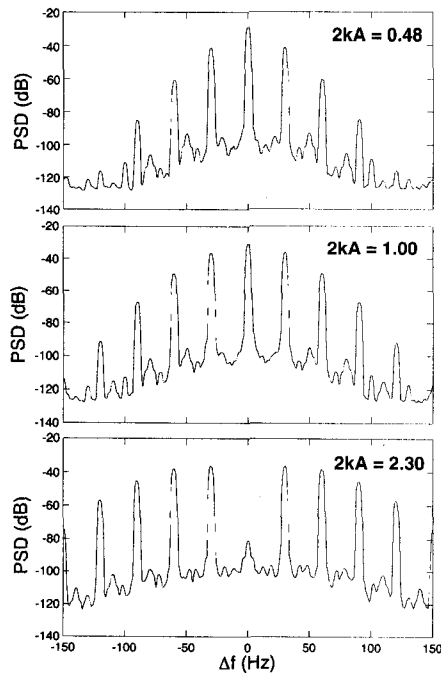


Fig. 1. Power spectra of the wave scattered by the vibrating plate at frequency $F = 30$ Hz as a function of the dimensionless vibration amplitude $2kA$ (k is the wave number of the incident high frequency wave, f). The x -axis represents the Doppler shift, such that the origin corresponds to $f = 2.25$ MHz.

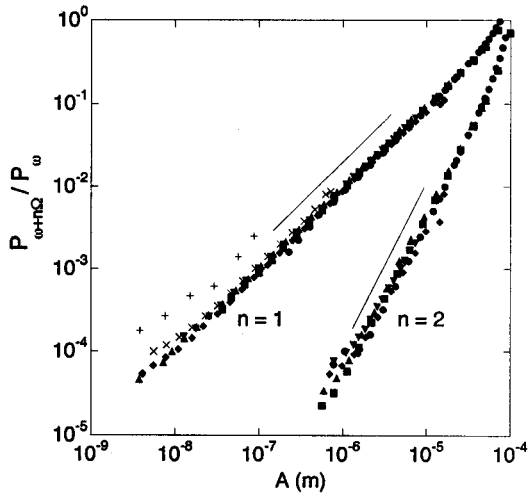


Fig. 2. Normalized amplitudes $P_{\omega+n\Omega}/P_{\omega}$ of the peaks at frequencies $f+nF$ ($n = 1, 2$) as a function of the vibration amplitude A : $F = 30$ Hz (\bullet), 60 Hz (\blacksquare), 120 Hz (\blacktriangle), 180 Hz (\blacklozenge), 700 Hz (\blacktriangledown), 3000 Hz (\times), 6000 Hz ($+$). Continuous lines display the slopes 1 and 2.

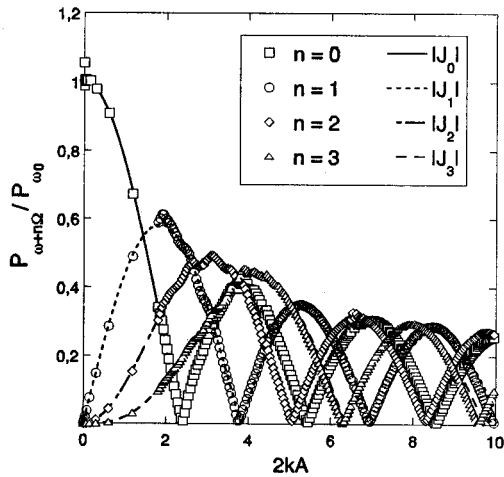


Fig. 3. Normalized amplitudes $P_{\omega+n\Omega}/P_{\omega_0}$ of the peaks at frequencies $f+nF$ ($n = 0, 1, 2, 3$) as a function of the dimensionless vibration amplitude $2kA$: $n = 0$ (\square), $n = 1$ (\circ), $n = 2$ (\diamond), $n = 3$ (\triangle). Lines display the moduli of Bessel functions of order n . P_{ω_0} is the amplitude of the reflected wave when the piston is at rest.

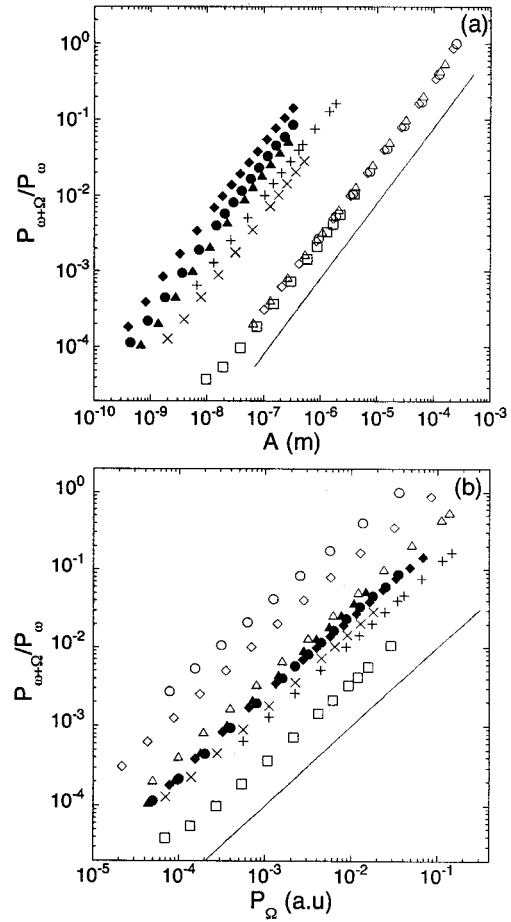


Fig. 4. Normalized amplitudes $P_{\omega+n\Omega}/P_{\omega}$ as a function of the vibration amplitude A (a) and as a function of the low frequency pressure P_{Ω} (b): $F = 30$ Hz (\circ), 60 Hz (\diamond), 120 Hz (\triangle), 964 Hz (\square), 1200 Hz ($+$), 3000 Hz (\times), 3500 Hz (\bullet), 4000 Hz (\blacklozenge), 4500 Hz (\blacktriangle) (Solid lines of slope one.)

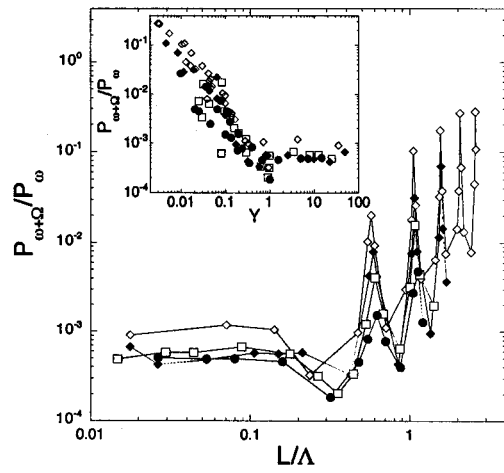


Fig. 5. Normalized amplitudes $P_{\omega+\Omega}/P_{\omega}$ as a function of L/Λ for $A = 0.22 \mu\text{m}$: $L = 20 \text{ cm}$ (\diamond), 30 cm (\blacklozenge), 50 cm (\square), 90 cm (\bullet). The inset displays the dependence of the same quantity on the dimensionless ratio $Y = 2\rho c^2 A / \epsilon L P_{\Omega}$.